

C/O Ratios and the formation of wide separation exoplanets

EDWIN A. BERGIN,¹ RICHARD A. BOOTH,² MARIA JOSE COLMENARES,¹ AND JOHN D. ILEE²

¹*Department of Astronomy, University of Michigan, 1085 S. University Ave, Ann Arbor, MI 48109, USA*

²*School of Physics and Astronomy, University of Leeds, Leeds, LS2 9JT, UK*

ABSTRACT

The gas and solid-state C/O ratios provide context to potentially link the atmospheric composition of planets to that of the natal disk. We provide a synthesis of extant estimates of the gaseous C/O and C/H ratios in planet-forming disks obtained primarily through analysis of Atacama Large Millimeter Array observations. These estimates are compared to atmospheric abundances of wide separation (> 10 au) gas giants. The resolved disk gas C/O ratios, from seven systems, generally exhibit $C/O \geq 1$ with subsolar, or depleted, carbon content. In contrast, wide separation gas giants have atmospheric C/O ratios that cluster near or slightly above the presumed stellar value with a range of elemental C/H. From the existing disk composition, we infer that the solid-state mm/cm-sized pebbles have a total C/O ratio (solid cores and ices) that is solar (stellar) in content. We explore simple models that reconstruct the exoplanet atmospheric composition from the disk, while accounting for silicate cloud formation in the planet atmosphere. If wide separate planets formed via the core-accretion mechanism, they must acquire their metals from pebble or planetesimal accretion. Further, the dispersion in giant planet C/H content is best matched by a disk composition with modest and variable factors of carbon depletion. An origin of the wide separation gas giants via gravitational instability cannot be ruled out as stellar C/O ratios should natively form in this scenario. However, the variation in planet metallicity with a stellar C/O ratio potentially presents challenges to these models.

1. INTRODUCTION

For the past decade there has been strong effort to explore the link between the exoplanetary atmospheric composition and the composition of its natal disk (see Öberg & Bergin 2021, and references therein). In part this has been motivated by the simple theory suggested by Öberg et al. (2011b). This theory assumes interstellar abundances to focus on the main elemental carriers of C and O (CO, CO₂, and H₂O). The overall chemistry in the low ionization state disk midplane (Umebayashi & Nakano 1988; Cleaves et al. 2013) dictates that sublimation alone is primarily responsible for changes in the ratio of carbon to oxygen in the ice versus gas as a function of stellar distance.

The relative balance of C/O between the gas and ice matters as within the core-accretion paradigm of giant planet formation, a many Earth-mass core forms from the icy solids. The H₂ dominated atmosphere *at birth* carries the composition of the gas at its formation distance. The corollary is that ices, and the Earth-size core, are oxygen rich. This may be more complicated as planets migrate, can capture icy planetesimals, and might have core-atmosphere mixing along with gravitational settling (Cridland et al. 2016; Helled & Guillot 2017; Guillot et al. 2022). However, it encapsulates a central element and is now widely compared to exoplanet atmospheric composition retrievals (Barman et al. 2015; Lavie

et al. 2017; Oreshenko et al. 2017, to list a few). As a corollary, an alternative route to formation would be direct gravitational collapse within an unstable disk (Boss 1997; Durisen et al. 2007). If this were to occur early, prior to significant grain growth within the disk, then a solar/interstellar composition would naively be predicted.

Observational constraints on the overall gas phase C/O ratio are obtained via analysis of data from the Atacama Large Millimeter Array (ALMA). In gaseous emission lines of molecules ALMA is capable of resolving disk systems with ~ 10 -15 au resolution (Öberg et al. 2021; Law et al. 2021) and numerous observational analyses have been undertaken to constrain the elemental C/O and C/H ratios in this gas (Miotello et al. 2022, and references therein). Many of these disk systems are suggested to be sites of incipient planet formation (Pinte et al. 2023; Bae et al. 2023, and references therein).

Concurrently, new instruments (e.g. JWST) and ground-based high resolution spectroscopy have opened a new era in precision measurements of the C/O ratio in planets at wide distances from their stars encompassing similar spatial scales as probed by ALMA (GRAVITY Collaboration et al. 2020; Wang et al. 2020; Mollière et al. 2020; Ruffio et al. 2021; Petrus et al. 2021). Thus, it is a fruitful time to revisit the current state of our understanding of C/O measurements within young (1-10 Myr-old) gas-rich protoplanetary disk systems

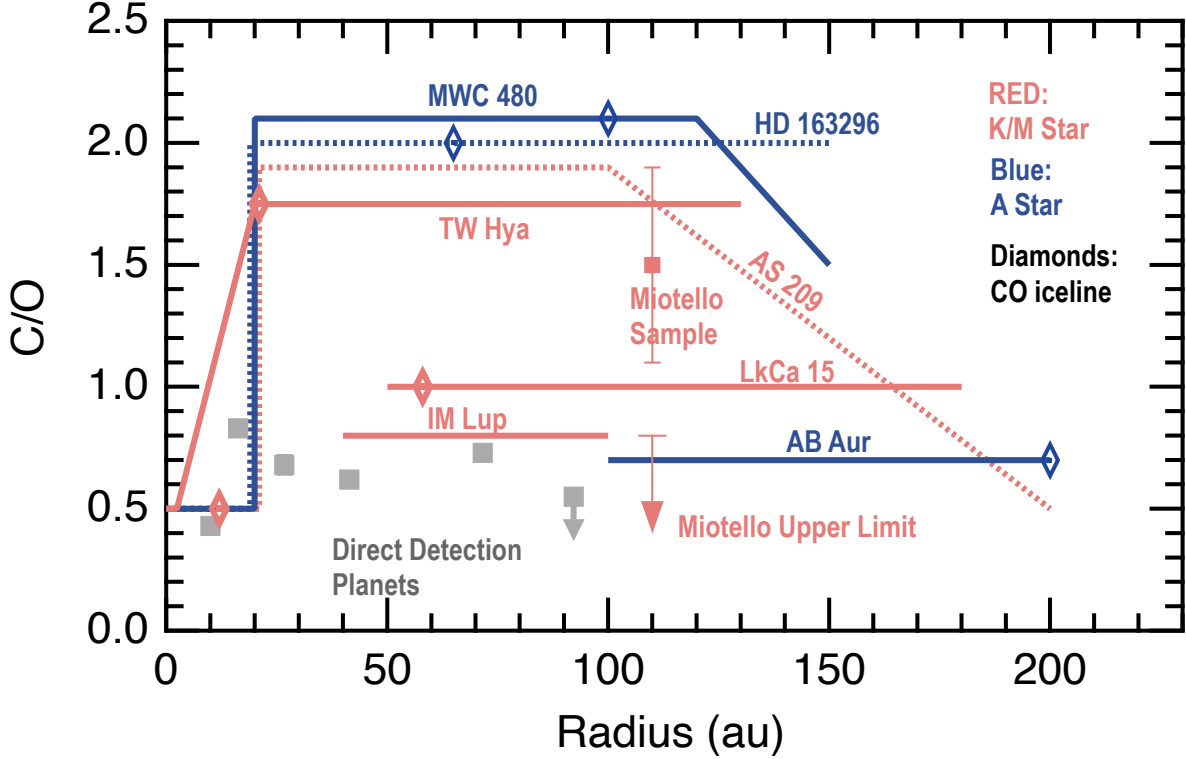


Figure 1. Radial distributions of derived C/O ratios in named disk systems from C_2H (Bergin et al. 2016; Kama et al. 2016; Cleeves et al. 2018; Bosman et al. 2022; Sturm et al. 2022) and CS/SO (Rivière-Marichalar et al. 2022). Also shown is the range of C/O ratios estimated by Miotello et al. (2019) in a survey of C_2H in Lupus disks. This survey had some lower limits which imply smaller disks or lower C/O ratios. In the figure A stars are shown in red and later spectral types in blue. The solid grey squares denote the estimated elemental C/O ratios towards direct detection planets β Pic B (GRAVITY Collaboration et al. 2020), HR8799bcde (Nasedkin et al. 2024), HIP 65426 b (Petrus et al. 2021). The *estimated* error bars for some of the planet C/O ratios are smaller than the marker size. The open diamonds superposed on a given C/O ratio line are the estimated location of the CO snowline for that object with references given in the Appendix. For AB Aur the CO snowline is located at $r > 200$ au and for IM Lup the CO snowline is near ~ 15 au.

in comparison to the composition of exo-giant planet atmospheres. In this paper we synthesize the observational state-of-the-art in linking disk and exoplanet atmospheric composition towards understanding the formation of wide separation planets in light of extant C/O ratio measurements. We summarize existing *resolved* C/O ratio measurements to provide an observationally constrained plot of the C/O ratio as a function of distance moving beyond the simple theory of Öberg et al. (2011b). As part of this effort, we discuss the methodology applied toward retrieval of C/O ratios from gas phase emission lines. Finally, we compare these results to extant measurements of C/O in the gas giant atmospheres and explore simple formation models to delineate what this comparison implies for the planet formation. In this work we adopt a solar C/O ratio of 0.55 ± 0.06 as our reference frame and in Appendix A we outline how this value relates to the often uncertain stellar reference value for these systems.

2. ALMA C/O MEASUREMENTS

The methodology to determine the C/O ratio from ALMA observations of molecular line is outlined in Appendix B. The majority of ALMA C/O ratio measurements are performed near and inside the CO snowline where the chemical expectation is that the carbon and oxygen in the gas are carried by CO, e.g. $C/O = 1$ (Öberg et al. 2011b). The spatial coverage encompasses two zones within the disk, these are: (1) just inside the CO snowline where gas potentially traces the planet-forming midplane and (2) radii beyond the CO snowline, where gas CO is found only in warm ($T > 20\text{--}30$ K) surface layers above the midplane where CO is presents as ice (Aikawa et al. 2002). For both regions the ratio can be indirectly measured using chemical systems that are both dependent on the elemental C/O ratio and have observable molecular transitions within the ALMA bandpasses. The chemical systems are via the emission of C_2H and $C^{18}O$ (Bergin et al. 2016; Kama et al. 2016) and the ratio of CS/SO (Semenov et al. 2018; Le Gal et al. 2021).

In Fig. 1 we present the C/O ratio measurements in 7 disk systems surrounding A stars (3) and K/M stars (4). In Appendix C we provide the source by source discussion of this measurement from molecular emission images. For simplicity we adopt solar abundances as our reference frame with a C/O ratio of ~ 0.55 ; this is discussed in Appendix A. Fig. 1 also shows the estimated CO snowline for resolved systems. The other relevant snowline on these spatial scales is CO₂. Assuming a CO₂ sublimation temperature of ~ 55 K (Minissale et al. 2022), we estimate (rough) CO₂ snowline locations of ~ 10 – 15 au for the Ae/Be systems (HD 163296 and MWC 480) and inside 3 au for the T Tauri disks (TW Hya, IM Lup, and AS 209). The CO₂ snowline lies inside the dust cavities of LkCa15 and Ab Aur. Based on this information the majority of measurements are nominally tracing material where the expectation value is C/O = 1 and ALMA measurements retrieve near this value in 3 instances (LkCa 15, IM Lup, and AB Aur) but in other disks the gas phase C/O is estimated to be > 1 beyond 20 au. Inside 20 au a lower ratio is inferred.

In Appendix D we also summarize estimates of the gas phase CO abundance in these disks which appears to be reduced compared to interstellar by ~ 10 or more (see source by source discussion in the Appendix and also Bergin & Williams 2017; Miotello et al. 2022). Since CO comprises nearly 50% of the available carbon (Bergin et al. 2015; Mishra & Li 2015) this is well below the expected value. Beyond the CO₂ snowline the abundance of CO is believed to trace the C/H content of planet-forming gas (Öberg et al. 2011b); thus, to date, most planet-forming disks have C/O $\gtrsim 1$ and C/H $< C/H(\text{solar})$ (Bosman et al. 2021b).

3. PLANET FORMATION AND C/O

3.1. General Implications

Fig. 1 also provides estimates of the atmospheric C/O ratio of wide separation gas giants illustrating a general mismatch between the C/O ratio measured in direct detection gas giants and the gas phase C/O in natal disk systems (discussed in Appendix E). Placing the focus on planet and disk material beyond 20 au the majority of disk systems subject to detailed chemical analyses have gas phase C/O ≥ 1 while planetary material appears closer to solar values. Another clear statement can be made from Fig. 1: if the disk gas phase C/O is greater than solar, and C/H is depleted by a factor of ~ 10 , then the ice coatings of the pebbles likely have solar composition. This is illustrated in Fig. 2 where we plot an estimate of the C/O ratio of the pebbles as a function of the overall depletion factor of carbon (traced by CO) and the gas-phase C/O ratio. Specifically, we define the depletion factor Δ_C relative to the volatile carbon content in the ISM (assumed to be half the solar carbon abundance, Mishra & Li 2015), such that $\Delta_C = 2$ implies that 1/4 of the carbon is in the

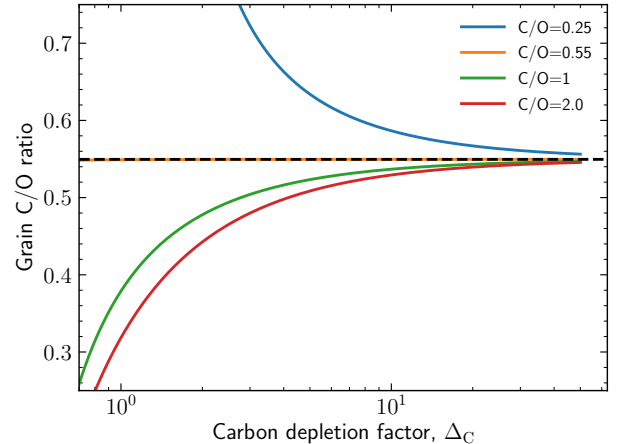


Figure 2. Estimated C/O ratio within the grain icy mantle and solid core as a function of the gas phase C/O ratio and the overall carbon depletion factor. Here we assume a solar composition for the stellar content. The dashed line represents the solar/stellar C/O ratio.

gas phase. If C/O ≥ 1 and $\Delta_C \sim 10$, then the icy grain mantle C/O ratio is close to solar in composition. That is the grains contain the majority of the solids (silicates, carbonaceous materials) and the volatiles (e.g. CO, H₂O, and CO₂).

There are two rough groupings of C/O within the disk systems with C/O = 1.5–2.0 (AS 209, HD 163296, TW Hya, and MWC 480) and those with C/O = 0.7–1.0 (LkCa 15, Ab Aur, IM Lup). This difference *could* be due to evolutionary differences as the latter sources are relatively young (1–5 Myr) while the former are generally older (> 5 Myr). However, this is not completely the case. AS 209 has been subject to two semi-independent chemical analyses (i.e., two different codes using the same baseline physical structure; Bosman et al. 2021b; Alarcón et al. 2021) has an elevated C/O ratio and is estimated to be a young (1–3 Myr old) system. Abundance evolution is inferred to be present for CO, the primary gaseous C/H carrier, over million year timescales (Bergner et al. 2019; Zhang et al. 2019), and the elevated C/O ratios may develop over similar timescales. Thus, chemical evolution with planet formation within a few Myr is one possibility.

3.2. The Focus on A Star Disks

An additional aspect is that the direct detection host stars are primarily A stars. In this case the comparison sample is HD 163296, MWC 480 and AB Aur. Again, age may play a factor as AB Aur is the youngest system and displays C/O ~ 0.7 – 1 (see Appendix C.3). In fact, Ab Aur is suggested to be accreting material from its natal cloud (Tang et al. 2012) and also hosts a potential protoplanet (Currie et al. 2022). The accretion of this fresh material may alter the C/O ra-

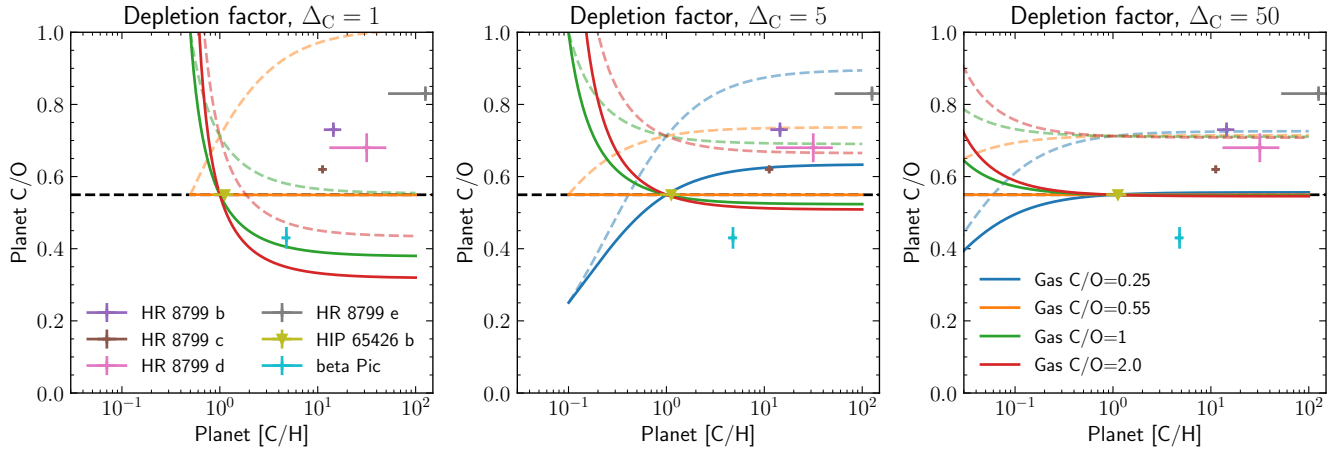


Figure 3. A comparison between the observed composition of planets (crosses) and the compositions obtained by combining different amounts of solids and gases (lines). The solid lines show the potential planet compositions for a given disk C/O ratio; in different panels, we have varied the amount of carbon depletion as in Fig. 2. The solid lines assume all material contributes to the planet’s composition, while the dashed lines assume that silicates condense out. For HIP 65426 b, the C/O ratio shown is the upper limit (Petruš et al. 2021).

tio in the disk gas. In general, we expect that material accreted from the surrounding cloud will have a composition consistent with interstellar gas and ices. These have CO in the gaseous state with most oxygen confined to the refractory cores of grains and in CO, CO₂, and water ice (Öberg et al. 2011a; McClure et al. 2023). To lower the C/O ratio below unity some of the oxygen trapped in CO₂ and H₂O ice needs to be released to the gas. There is some evidence of chemical changes associated with accretion in protostars which have strong SO and SO₂ emission sometimes spatially associated with a young protostellar disk (Sakai et al. 2014; Artur de la Villarmois et al. 2022; Flores et al. 2023; Kido et al. 2023). The presence of these oxygen-rich sulfur-bearing species is suggestive that some oxygen is returned to the gas, a facet that is consistent with models (Miura et al. 2017; van Gelder et al. 2021).

However, we have no information regarding the C/O ratio for Ab Aur inside 100 au. Thus, it is not clear that age is an issue. The systems where we do have information that is spatially coincident with the direct detection exoplanet population is MWC 480 and HD 163296. In both systems beyond 20 au the gaseous C/O ratio is elevated near 2 and well above the values inferred in the exoplanet atmospheres. Inside 20 au the situation is less clear. HD 163296 provides the best information via the rotational emissions of CH₃CN and HC₃N which peak near 40 au (Ilee et al. 2021) and decay towards smaller radii. This is interpreted by Calahan et al. (2023) as a reset in the C/O ratio, but this is uncertain. What is clearer is the fact that gaseous C/O ratio beyond 20 au in most disk systems appears to be elevated above that measured in the direct detection planets.

4. DISCUSSION

Current estimates clearly suggest a mismatch between the gas-phase C/O ratios measured in disk systems and that in exoplanet atmospheres. Below we focus on simple models of planet formation that encompass the disk gas phase C/O and C/H constraints (with the implication that constraining both of these quantities in the gas also implies an O/H ratio) and explore how these might be consistent with existing exoplanet atmospheric constraints.

4.1. Modes of Planet Formation

We consider that the composition of the wide orbit giants is likely controlled by the composition and relative amount of gas and dust accreted. Using the gas abundances derived for the outer regions of protoplanetary disks and the compositions of wide-orbit giants (see Table 1) that likely formed in these regions, we can begin to understand how these planets may have formed.

Our model methodology is given in Appendix F. We first consider the case where the total abundances of the gas and solids in the disk add up to the stellar abundances, for which we use the proto-solar abundances (Asplund et al. 2009) as a proxy. Partitioning the abundances based on the C/O ratio of the gas and the amount of carbon depletion, we then compute possible compositions for the planets by varying the amount of solid material accreted, with the results for typical C/O ratios and carbon depletions shown in Fig. 3. Increasing the amount of solids in the planet increases the planet’s carbon abundance $[C/H]$ and drives the C/O ratio towards that of the solids. In these solutions, disks with significant carbon depletion are generally preferred. In drawing this conclusion, we have accounted for the condensation of silicate clouds in the HR 8799, which raises the C/O ratio of the atmosphere because oxygen is locked up in silicates. See Appendix E

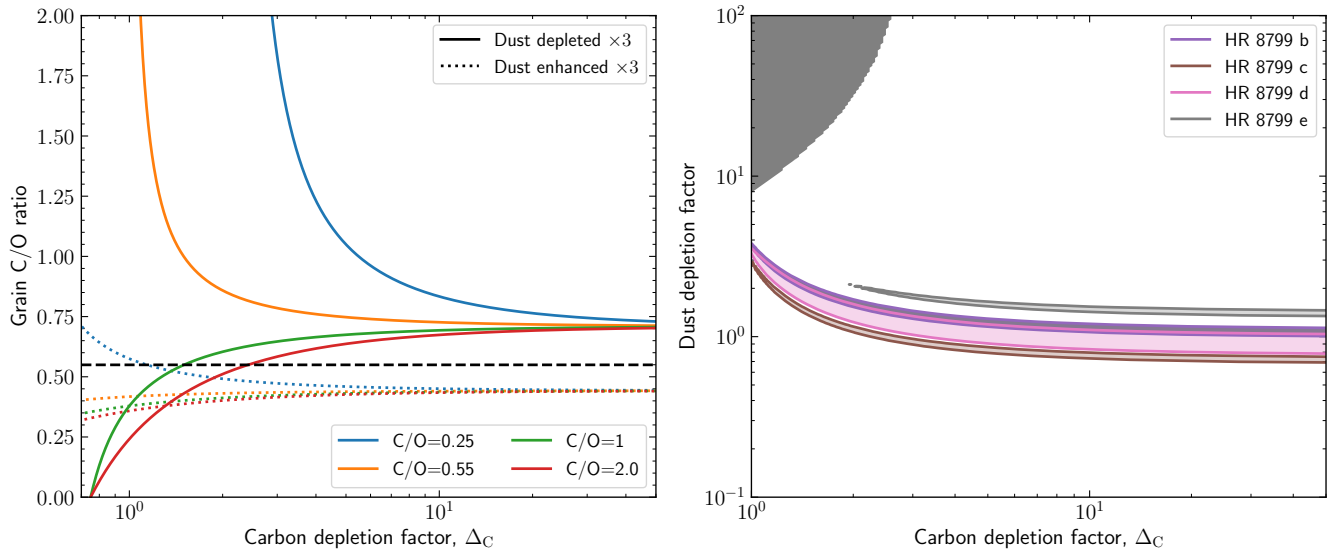


Figure 4. Left: Estimated C/O of the dust, as in Fig 2 but considering a depletion (solid lines) or enhancement (dotted lines) of icy material before chemical evolution alters the disk composition. The black line represents the solar ratio. Right: Constraints on the level of carbon depletion and dust depletion provided by the planets in the HR 8799 system, assuming the gas has a C/O ratio of 2. The filled regions in the contours show the regions where the disks can produce planets that match the observed composition to within 1σ , under the assumption that silicates condense into clouds and do not contribute to the observed composition. Note that a dust depletion smaller than one means that the dust-to-gas ratio has been increased. The other planets in Table 1 provide similar, but weaker constraints.

and Nasedkin et al. (2024), for a discussion. A corollary is the planets must have acquired most of their metals through the accretion of solids. The one exception is β Pic b, for which the high C/H and low C/O ratio prefer a low carbon depletion.

Increasing the amount of solids in the planet increases the planet’s carbon abundance [C/H] and drives the C/O ratio towards that of the solids. In these solutions, disks with significant carbon depletion are generally preferred. This is because the planets have a wide range of C/H ratios, but C/O ratios that are close to solar. This requires some variability in the C/H disk content. A corollary is the planets must have acquired most of their metals through the accretion of solids. The one exception is β Pic b, for which the high C/H and low C/O ratio prefer a low carbon depletion.

Alternatively, the HR 8799 and HIP 65426 b planets’ composition could be explained by any level of carbon depletion if the C/O ratio of the gas is close to the solar value. In this case, both the dust and gas have similar compositions, and the only planet formation outcome possible is a C/O the solar value. Only AB Aur has a C/O ratio close to solar, however, and this is the youngest disk. This suggests an alternative explanation for the composition of the planets, which is that they formed early, before chemical evolution was significantly underway.

4.2. Gas and Dust Separation

Since the composition of ice in these disks is not known, we cannot be certain that the total abundance of gas and

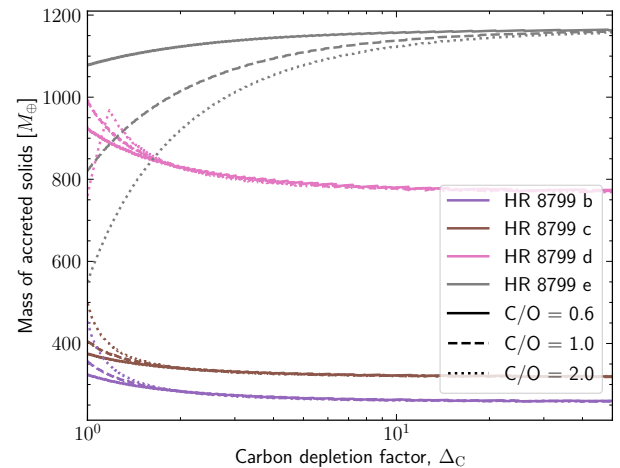


Figure 5. Estimated mass of accreted solids from simple model as a function of the carbon depletion factor (Δ_C) and the dust depletion factor. The dust depletion factor was chosen to be the best fit value based on the C/H of the planets, and it corresponds to ~ 0.5 – 5 , depending on the assumed C/O ratio. When the dust depletion factor is less than one it reflects a local dust enhancement.

solids is solar. A non-solar total abundance requires that the dust and gas evolve separately, but processes such as radial drift or dust trapping in sub-structures can affect the disk composition by removing or enhancing the amount of ice (Pinilla et al. 2017; Kalyaan et al. 2023). Based on ALMA observations, it is clear that in many disks the outer gaseous radii are much larger than the mm-sized dust (Ansdell et al.

2018; Sanchis et al. 2021) which demonstrates that some gas exists in regions where dust is depleted. This would not alter our conclusions above if the dust evolution happens after the chemical evolution. However, there is good evidence that the dust could evolve more quickly. For example, sub-structures are seen at all ages (Huang et al. 2018), and theory predicts that dust will evolve rapidly in their absence.

To estimate how differences in the gas and dust evolution affect the composition of the solids we need to know how much material is lost together with its composition. We assume that any dust evolution happens while the disk has its initial composition; this choice maximizes the impact of dust evolution if the gas composition evolves monotonically everywhere in the disk. The initial composition is assumed to be inherited from the interstellar medium, in which approximately 50% of the carbon is in the form of CO (Mishra & Li 2015). In the cold outer regions probed by the ALMA observations, all other major carbon and oxygen carriers will be in the form of ice. From this, we can estimate the carbon and oxygen abundance of the ice by first computing a new total abundance from the gas-phase CO abundance plus the dust abundances divided by a *dust* depletion factor (which could reflect a true depletion or an enhancement in a trap). The final dust abundance is then computed by assuming this new total composition is partitioned between the gas and dust according to the observed C/O ratio and carbon depletion factor. We show how this affects the composition of the grains in Fig. 4. When dust enhancement occurs (e.g. via dust trapping), the final composition of the grains is closer to their ISM abundance ($C/O \approx 0.38$) as the gas is less important. Dust depletion has the opposite effect, with the dust’s initial contribution being smaller, increasing the dust’s C/O ratio towards unity (since the gas contained only CO).

Ultimately, it is likely that the C/O ratio of protoplanetary disk dust is not too different from solar when most of the planets formed. Our models predict only a small change in the solid C/O ratio of the disk for reasonable changes in the amount of dust ($\lesssim 0.1$ for $0.3 \lesssim \Delta_d \lesssim 3$, Fig. 4, left panel), and the inferred compositions of the planets in HR 8799 favor little-to-no change in the amount of dust (Fig. 4, right panel). While we have only included HR 8799 planets, HIP 65426 b provides consistent, albeit weaker, constraints. This confirms our previous statement that the planet’s compositions prefer a modest level of carbon depletion in the disk unless the planets formed early, when the disk had a low C/O prior to significant dust evolution. β Pic b is again an exception in this regard, with the planet’s low C/O and high C/H ratios either favoring no depletion and a gas phase $C/O \approx 1$ (Fig. 3) or a dust enhancement.

4.3. Metal Enrichment of Planet Envelope

Giant planet formation models based on planetesimal accretion, pebble accretion, and gravitational instability differ in their predictions for the amount of solids accreted. In Fig. 5, we show the amount of solids the HR 8799 planets must have accreted to match the metallicity and C/O ratios inferred by Nasedkin et al. (2024), assuming the best-fit dust depletion factor for each Δ_C . These high metallicities inferred for the HR 8799 planets by Nasedkin et al. (2024) imply the accretion of several $100 M_{\oplus}$ to $1000 M_{\oplus}$ of solids to match the observed composition. The total solids in all of the HR 8799 planets exceed $2000 M_{\oplus}$ and is comparable to the amount of dust in a solar mass of solar-composition gas.

It is unlikely that any standard planet formation scenario can explain these abundances. Pebble accretion is expected to stop once a planet reaches the pebble isolation mass and the pebble isolation mass is unlikely to exceed $\sim 100 M_{\oplus}$ (Bitsch et al. 2018), ruling out pebble accretion as a mechanism to explain these metallicities. Similarly, there is unlikely sufficient mass in planetesimals to explain the metallicities. While gravitational instability can also produce super-solar metallicities if dust concentrates in the spirals before collapse (Boley & Durisen 2010), metallicities above a few times solar have not yet been seen in simulations. As a result, no known formation pathway naturally explains the high metallicities inferred for these massive planets.

Estimates of the solid abundance based on previous studies (e.g. Mollière et al. 2020; Ruffio et al. 2021; Wang et al. 2020) produce abundances that are a factor ~ 10 lower (Mollière et al. 2020) due to the lower metallicity ($\lesssim 3$ times solar) inferred by these studies. These lower abundances are less problematic, and each formation scenario could likely achieve them.

Putting aside the question of how the very high metallicities can be achieved, we address what the planets’ compositions tell us about how the planets formed. Fig. 4 tells us that the HR 8799 planets likely formed in a disc with a modest level of gas-phase carbon depletion and solids that had a composition close to solar if silicates are condensing in the planet’s atmospheres.

Planetesimal accretion models are consistent with the C/O ratios in the HR 8799 planets when considering the carbon depletion seen in disc observations. The main challenge for planetesimal accretion would be explaining the overall metallicity and mass-metallicity trends in the HR 8799 system. Planetesimal accretion models predict anti-correlated mass-metallicity relations (e.g. Thorngren et al. 2016; Mordasini et al. 2016), but the HR 8799 planets do not follow this.

The main challenges for forming the HR 8799 planets by pebble accretion are 1) explaining how the pebbles ended up enriching the planet’s atmosphere since they would have been accreted while the planet was less than the pebble isolation mass and thus before the planet accreted most of the

gas. These pebbles would initially form a dilute core that would have to be mixed into the atmosphere to contribute to the current day planet abundances (Ormel et al. 2021). 2) Demonstrating that giant, metal-rich planets can form without the drifting pebbles enriching the disk gas, since large enrichments produce planets with $C/O \sim 1$ and disks with $[C/H] \gtrsim 1$ (Booth et al. 2017; Booth & Ilee 2019; Danti et al. 2023).

It is also difficult to reconcile the HR 8799 planets’ abundances with formation via gravitational instability since the abundances require some level of carbon depletion or dust depletion (Fig. 4) and this is not expected to occur in the short period of time when gravitational instability is viable. However, gravitational instability takes place in an extremely dynamic disc, which can affect the disc’s composition (Ilee et al. 2017); the impact of these effects on the planets’ composition are currently unknown. Condensation and settling of grains within a fragment would affect the composition too, as would the subsequent removal of the gaseous envelope (so called tidal stripping or downsizing) would also result in objects with higher metallicity (Boley & Durisen 2010; Nayakshin 2010) and different elemental ratios (e.g. Ilee et al. 2017).

Here, we have focused on the composition of the HR 8799 planets because they provide the most challenges. Of the other planets considered, HIP 65426 b has been inferred to have a composition close to solar, which is compatible with essentially all formation scenarios. β Pic b would also likely be compatible with any formation channel if it formed early, when $\Delta_C \approx 1$ and $C/O = 1$ are expected in the outer parts of the disc.

5. SUMMARY

We present a synthesis analysis of the C/O ratio in the outer regions of gas-rich protoplanetary disks in comparison to that found in wide separation exoplanet atmospheres. This comparison leads towards a number of conclusions.

1. The disk resolved gaseous C/O ratio from seven disk systems has $C/O \geq 1$ with subsolar C/H content. These measurements correspond to disk locations where the baseline chemical expectation is $C/O = 1$.
2. Within this sample the youngest sources appear to have the lowest C/O ratios which tentatively (small sample of systems) hints at chemical evolution in the overall C/O ratio, which may be commensurate with similar

evolution in C/H (Bergner et al. 2019; Zhang et al. 2019).

3. Based on the gas phase C/O and C/H values inferred for the gas we conclude that the total C/O ratio of pebbles in planet-forming disks, including the solid cores and the ice mantles, have a C/O ratio that is solar in content. The results from the ALMA large program “The Disk Exoplanet C/Onnection” (DECO), will provide the needed statistics to confirm these conclusions.
4. Disk C/O ratios are uniformly above that measured in wide separation exoplanet atmospheres where the ratio is closer to solar or stellar (where known). Using a simple analysis based on the constraints of the gaseous and solid state composition we show that the exoplanet composition can be matched provided that pebbles provide the bulk of planet metals. As an additional constraint the dispersion in giant planet atmospheric carbon content (e.g. C/H) requires a modest level of carbon depletion in disk gas.
5. Based on this comparison we cannot conclude on the primary method of planet formation whether gravitational instability or core accretion. However, we do note that the youngest disk sources have the lowest C/O ratios. This may favor a solution where planets form early before significant chemical evolution ensues. However, if the range in the C/H content in exoplanet atmospheres is correct then the dual constraints of requiring solar/stellar C/O and variable C/H challenges some solutions.

We are grateful to a thorough and constructive review from an anonymous referee which improved this manuscript. E.A.B. acknowledges support from NSF grant No. 1907653 and NASA NASA’s Emerging Worlds Program, grant 80NSSC20K0333, and Exoplanets Research Program, grant 80NSSC20K0259. R.A.B. thanks the Royal Society for their support via a University Research Fellowship. J.D.I. acknowledges support from an STFC Ernest Rutherford Fellowship (ST/W004119/1) and a University Academic Fellowship from the University of Leeds.

Facilities: ALMA, NOEMA

Software: astropy (Astropy Collaboration et al. 2013, 2018),

APPENDIX

A. INTERSTELLAR REFERENCE C/O VS STELLAR C/O

All of the young disks in our discussion are within ~ 150 pc and have formed from local interstellar medium gas. The C/O ratio of this gas has been estimated through the determination of photospheric abundances of early type B-stars in OB associations (Nieva & Przybilla 2012) and this reference value is $C/O = 0.37 \pm 0.06$. This is in comparison to the solar value of 0.51 ± 0.06 using the most recent solar oxygen (Bergemann et al. 2021) and carbon (Asplund et al. 2021) abundance estimates. The solar value represents the local ISM circa 4.6 Billion years ago and the differences potentially represent galactic chemical evolution in that time span. However, the error estimates between the interstellar value and the solar value overlap and for our purposes we adopt the solar value as a reference value. Further, in this work we use the solar composition reported in Asplund et al. (2009) with $C/O = 0.55 \pm 0.06$ as this value is widely used in the literature and its use provides a common reference point for comparison to earlier works.

The direct detection planets stellar C/O ratios are not always known. However, Wang et al. (2020) estimate a stellar C/O ratio of $0.54^{+0.12}_{-0.09}$ for HR8799. More generally, Biazzo et al. (2022) surveyed the stellar abundances of transiting exoplanet host stars finding that all host stars have $C/O < 0.8$ with peak values in two metallicity bins, $Z_{\star}/Z_{\odot} \leq 1.3$ and > 1.3 , of ~ 0.45 and 0.5 , respectively. In sum, while there is uncertainty, the expectation is that the stellar value is close to 0.5 or slightly below. Certainly the variation in the estimated C/O ratio in HR8799 (Nasedkin et al. 2024) seen in Fig. 1, if supported by future work, is suggestive of planetary deviations from stellar.

B. OUTLINE OF METHODOLOGY TO DERIVE C/O FROM ALMA OBSERVATIONS

B.1. C_2H and $C^{18}O$

C_2H emission is noted as unusually strong in disk systems with emission levels rising to be commensurate with ^{13}CO in some instances (Kastner et al. 2014). The C/O ratio is estimated using this tracer via forward-modeling of individual systems through detailed (thermo-)chemical models. The first step involves fitting the overall dust spectral energy distribution from near-IR to mm wavelengths alongside the resolved flux distribution of the dust sub-millimeter emission within the framework of known stellar parameters (accretion rate, stellar mass/radii, and luminosity) with parametric models of the distribution of the dust density both radially and vertically (Andrews 2020). Radiation transfer within the mass distribution, with assumed dust properties (Pollack et al. 1987; Birnstiel et al. 2018), sets the temperature distribution of the dust disk. Based on observations, the majority of the dust mass resides in the midplane held by larger mm-sized grains with smaller grains coupled to the gas following the flaring of the gaseous disk set by hydrostatic equilibrium (Dutrey et al. 2017; Villenave et al. 2020). Thermochemical models, which simultaneously simulate the chemistry and molecular line cooling, are used to solve for the thermal and chemical properties of surface layers where the dust and gas temperatures diverge (Woitke et al. 2009; Gorti et al. 2011; Bruderer et al. 2012; Du & Bergin 2014).

Models generally first match the distribution of $C^{18}O$. In this framework the gas mass and the CO abundance are degenerate (e.g., Calahan et al. 2021). The overall abundance of CO is an important issue and is effectively set via assumptions about the disk gas mass. In these models, the CO abundance effectively sets C/H (and O/H) in the gas beyond the CO_2 iceline. In this paper we will report CO abundances as measured in the given paper and refer the reader to the summaries in Bergin & Williams (2017) and Miotello et al. (2022). With the CO abundance set, the overall elemental C/O ratio is varied by adding excess carbon (in the form of C I or CH_4) and matching the level of C_2H emission and/or estimated column density. This gives leverage for the C/O ratio from the assumed value of 1 and above. Since C_2H is a tracer of UV illuminated gas (Nagy et al. 2015) there is an additional dependence on the amount of small grains present in surface layers (Bosman et al. 2021b). There are two variations to this method. Cleeves et al. (2018) traced C/O ratios below unity by adding additional water ice into the model which can be photodesorbed to provide gas phase oxygen to destroy C_2H . Finally, Calahan et al. (2023) extended tracers of C/O to include the overall complex carbon chemistry through the emission of CH_3CN and HC_3N ; HCN is also used (Cleeves et al. 2018; Rivière-Marichalar et al. 2020). For additional information the reader is referred to the discussion in Fedele & Favre (2020).

B.2. CS and SO

The CS/SO ratio in existing measurements also currently probes gas beyond the CO_2 snowline. This chemical system has long been posited as a sensitive probe of the C/O ratio in dense interstellar medium gas (Bergin et al. 1997; Nilsson et al. 2000) as oxygen rich gas readily forms SO, while carbon-rich material favors the formation of CS over SO. Semenov et al. (2018) and Le Gal et al. (2021) demonstrate that this ratio maintains its effectiveness as a probe of C/O in disk systems. The methodology for the derivation of C/O is similar to that of C_2H in terms of model development with one key caveat: in comparison to C_2H the ratio of CS to SO is mass-independent requiring only detection or limits on the emission of CS and SO. We note that in some instances there are indications of non-axisymmetric structure in the emission of SO, hinting at localized variations in the C/O

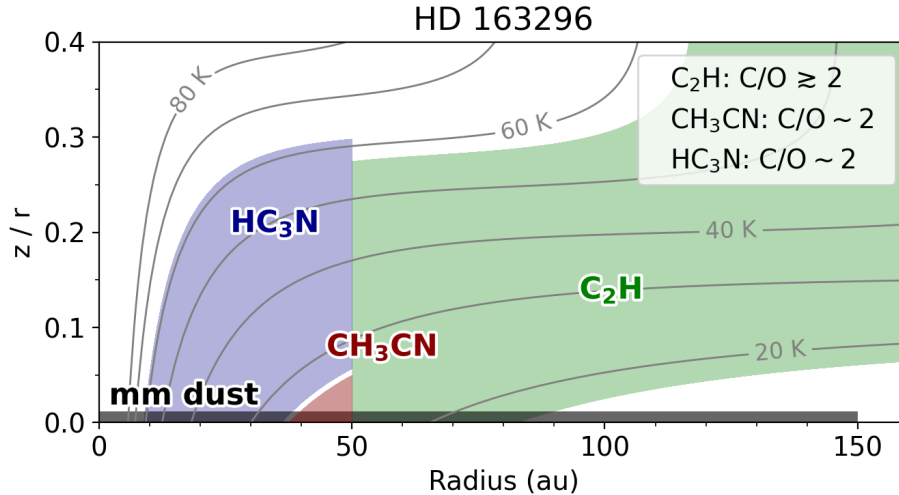


Figure 6. Origin of the line emission in the HD 163296 disk as determined in Guzmán et al. (2021) and Ilee et al. (2021). Also shown are the approximate C/O ratios derived from the analysis of Bosman et al. (2021a, from C₂H) and also Calahan et al. (2023, from CH₃CN and HC₃N).

ratio (e.g., Booth et al. 2023; Keyte et al. 2023). In this paper we discuss the majority of systems where, at present, emission appears to be symmetric and tracing the generic state of planet-forming material.

B.3. Comparison of Methods

Of the disk C/O ratio estimates shown in Fig. 1, AB Aur is the only one to have its C/O determined via CS/SO. All other C/O estimates were determined using C₂H and CO. Thus, it is possible that there could be a systematic effect between the two different methodologies. In this sample the only example where both have been used is towards MWC 480 where the spatial distribution of gas-phase CS and C₂H is constrained (Law et al. 2021; Guzmán et al. 2021; Le Gal et al. 2021), alongside an upper limit to the emission distribution of SO (Le Gal et al. 2021). In this regard the CS/SO limit is consistent with C/O > 0.9 in the same gas where C/O is estimated to be ~2 from C₂H. Thus, there is some baseline consistency, but clearly more work in this space is needed.

C. DESCRIPTION OF SOURCE SPECIFIC C/O MEASUREMENTS

C.1. HD 163296

HD 163296 is an A star ($M = 1.9 \pm 0.1 M_{\odot}$) with a luminosity of $17 L_{\odot}$ located at a distance of 101 pc (Fairlamb et al. 2015; Gaia Collaboration et al. 2018). The age of this system is estimated to be of order 5-7 Myr (Montesinos et al. 2009; Fairlamb et al. 2015). The C/O ratio in this system is measured by Bosman et al. (2021b) by matching C₂H and C¹⁸O emission. The ratio is estimated to be ≥ 2 beyond 50 au. Inside 50 au there is a decrease in the C₂H column. This rise does not appear to occur at the CO ice line, provided that its sublimation temperature is 22 K (Harsono et al. 2015; Bosman et al. 2021b). Calahan et al. (2023) use CH₃CN and HC₃N emission to estimate C/O in the inner 50 au for HD 163296. They show that the C/O ratio is comparable to C₂H from 20-50 au but must decline in the inner 20 au. We follow their suggestion of C/O = solar in this gas. Figure 6 gives an overview of the radii and relative heights in the disk that are probed by these observations. This figure illustrates that, for this system at least, the elevated C/O ratios extend closer to the star and trace both surface layers (HC₃N and C₂H) and material near the midplane as CH₃CN emission must arise from cold gas deep inside the disk (Ilee et al. 2021; Guzmán et al. 2021; Calahan et al. 2023). The CO abundance (C/H) beyond 100 au is of order 10^{-5} (Zhang et al. 2021) and potentially increases to super-solar in the inner tens of au (Zhang et al. 2020, 2021). The CO snowline is estimated to lie at 100 au by Zhang et al. (2021) based on CO isotopologue emission.

C.2. MWC 480

MWC 480 or HD 31648 is an A5-A6 star ($M = 1.85^{+0.04}_{-0.01} M_{\odot}$) with a luminosity of $16.6 L_{\odot}$ located at a distance of 162 pc (Gaia Collaboration et al. 2018; Guzmán-Díaz et al. 2021). The age of this system is estimated to be 6-7 Myr (Montesinos et al. 2009; Guzmán-Díaz et al. 2021). The C/O ratio in this system is measured by Bosman et al. (2021b) by matching C₂H and C¹⁸O

emission to find $C/O \geq 2$ beyond 40 au. The C_2H column exhibits a strong decline beyond 120 au which is interpreted as a change in the C/O ratio, and we place a smooth gradient in the plot to trace this decline. The C/O gradient beyond 120 au and this interpretation are highly uncertain. In the inner 40 au the C_2H column exhibits a decline. As in HD 163296 this decline lies inside the estimated location of the CO snowline. We place the reset of the C/O ratio to solar near 20 au based on the strong CH_3CN emission inside 40 au (Ilee et al. 2021). The late stage chemistry with an elevated C/O ratio invoked by Calahan et al. (2023) for HD 163296 is likely relevant for MWC 480. Thus we assume that a shift to lower C/O occurs closer to the star inside 20 au. The CO abundance (C/H) beyond 80 au is of order $\sim 5 \times 10^{-6}$ and potentially increases to solar or super-solar in the inner tens of au (Zhang et al. 2021). The CO snowline is estimated to be found near 65 au by Zhang et al. (2021) based on analysis of CO isotopologue emission.

C.3. AB Aur

AB Aur is an A1-A2 star ($M = 2.36_{-0.05}^{+0.4} M_\odot$) with a luminosity of $45.7 L_\odot$ at a distance of 163 pc (Gaia Collaboration et al. 2018; Guzmán-Díaz et al. 2021). Its age is suggested to be ~ 4 Myr (Guzmán-Díaz et al. 2021). Pacheco-Vázquez et al. (2016) detected SO emission within the disk and subsequent observations by Rivière-Marichalar et al. (2020) show that SO emission is confined to within a ring corresponding to 100 au and extending to larger distances. There is no CS measurement in this system and Rivière-Marichalar et al. (2020) find solutions that match current constraints with $C/O=0.7$ and $C/O=1$. We adopt $C/O=0.7$ for display in Fig. 1. The CO emission in the ring implies a gas-to-dust mass ratio of ~ 40 (Rivière-Marichalar et al. 2020); this could be consistent with gas loss from the canonical factor of 100 in the interstellar medium or a small reduction in the CO gas phase abundance. The models of Rivière-Marichalar et al. (2020) and Rivière-Marichalar et al. (2022) described above suggest a snowline location beyond 200 au in this source.

C.4. TW Hya

TW Hya is the closest young planet-forming disk system at a distance of 59.5 pc (Gaia Collaboration et al. 2016). The spectral type is M0.5 ($M = 0.6 \pm 0.1 M_\odot$) with a luminosity of $L = 0.26 L_\odot$ (Sokal et al. 2018; Herczeg & Hillenbrand 2014). The age of this system is debated (Debes et al. 2013; Herczeg & Hillenbrand 2014); we list here the most recent estimate of 5-11 Myr (Sokal et al. 2018). The C/O ratio in TW Hya is estimated via a variety of means. Bergin et al. (2016) and Kama et al. (2016) utilize C_2H emission to estimate 1.5-2.0 (we adopt 1.75). C_2H emission in this system is found in a ring extending from $\sim 20 - 100$ au (Kastner et al. 2015; Bergin et al. 2016). Cleeves et al. (2021) presented detailed observations of C_3H_2 which traces comparable chemistry to C_2H and demonstrate that the elevated C/O ratio extends from 30 au to ~ 120 au. Lee et al. (2021) discuss how the $^{14}N/^{15}N$ ratio observed in HCN has a dependence on the C/O ratio and suggest that $C/O > 1$ extends into 20 au. Interior to 20 au observations of water vapor and other tracers from Spitzer (Carr & Najita 2011) which were analyzed by Bosman & Banzatti (2019). They find depleted carbon and oxygen in the inner 2.4 au with an overall solar C/O ratio. We fix C/O to 1.75 into 20 au and to solar inside 2.4 au. This is also supported by analysis of abundances inside the silicate sublimation zone by McClure et al. (2020). The connection between these two levels is uncertain. The C/H abundance as traced by CO is of order 10^{-6} interior and beyond the CO snowline (Zhang et al. 2019; Yoshida et al. 2022a). The snowline in this system is based on the $^{13}C^{18}O$ emission and is suggested to lie near 21 au (Zhang et al. 2017).

C.5. LkCa 15

LkCa 15 is a K5 star ($M = 1.03 M_\odot$) with a stellar luminosity of $1 L_\odot$, an estimated age of 1-5 Myr (Simon et al. 2019; Donati et al. 2019; Pegues et al. 2020), and is located at a distance of 159.2 ± 1.2 pc (Gaia Collaboration et al. 2018). This disk holds a large inner gap out to ~ 50 au (Piétu et al. 2006; Facchini et al. 2020). Sturm et al. (2022) use C_2H to determine a C/O ratio of unity and a CO (C/H) abundance of $3.0 \pm 1.5 \times 10^{-5}$ from 50 au and beyond. This CO abundance is at least a factor of 3 depleted relative to the general ISM CO abundance (see Bergin & Williams 2017, for discussion of ISM CO abundance). Sturm et al. (2022) and Qi et al. (2019) estimate the CO snowline to lie near 58 au in this disk based on analysis of CO and N_2H^+ emission.

C.6. IM Lup

IM Lup (Sz82) is a K5 star ($M = 1.1 M_\odot$) with a stellar luminosity of $2.57 L_\odot$ at a distance of 158 pc (Alcalá et al. 2017; Gaia Collaboration et al. 2018; Öberg et al. 2021). This system is generally estimated to have a young age of order 1-3 Myr (Pinte et al. 2008; Alcalá et al. 2017). Cleeves et al. (2016) and Cleeves et al. (2018) explored the overall physical structure and C/O ratio in this system, respectively. The C/O ratio is generally estimated from C_2H but also is constrained via HCN observations, with an underpinning from CO isotopologue observations. Most efforts to determine the C/O ratio from C_2H utilize a coarse grid ranging from 0.5, 1, to > 1 . In this effort Cleeves et al. (2018) allowed for the presence of water ice in upper layers to provide oxygen

(via photodesorption) to the system and suggesting that this provides needed dynamic range between 0.5 and 1. The best fit was obtained between 40 to 100 au with $C/O = 0.8$. The inner tens of au of the IM Lup disk are obscured by strong dust continuum emission (Cleeves et al. 2016). The CO abundance (C/H) is estimated to be depleted by factors of 10-100 throughout the disk (Cleeves et al. 2016; Zhang et al. 2021). The CO snowline is found near 15 au based on analysis of CO isotopologue emission by Zhang et al. (2021).

C.7. AS 209

AS 209 is a K5 star ($M = 1.2 M_{\odot}$; $d = 121$ pc) with a stellar luminosity of $1.4 L_{\odot}$ and an estimated age of 1-3 Myr (Gaia Collaboration et al. 2018; Andrews et al. 2018; Huang et al. 2018; Avenhaus et al. 2018; Öberg et al. 2021). The C/O ratio was estimated via C_2H by Bosman et al. (2021b) and Alarcón et al. (2021). These works used independent codes but the same baseline physical model of the disk (taken from Zhang et al. 2021). Inside 10-20 au the drop in C_2H emission is interpreted as a drop in C/O towards 0.5. Similarly, the C_2H emission exhibits a sharp drop in intensity beyond 100 au which can be modeled with decrease of C/O to 0.5. Inside 20-100 au the C/O ratio is estimated to be ~ 1.9 . There is potential radial structure in the C/H or CO abundance. Zhang et al. (2021) and Alarcón et al. (2021) suggest that the CO abundance is depleted by about a factor of 10 within the inner 100 au but rises to a factor a few depletion near 150 au and declines towards the outer disk. The CO snowline is estimated to lie near 12 au based on analysis of CO isotopologue emission by Zhang et al. (2021).

C.8. Miotello C_2H Sample

Miotello et al. (2019) searched for C_2H emission towards a sample of disks with strong ^{13}CO emission isolated in the Lupus survey by Ansdell et al. (2016). In a total of nine targets C_2H emission was detected towards seven sources. Miotello et al. (2019) performed generic modeling of this sample to generate a relation between C_2H integrated flux density, disk mass, and overall C/O ratio. The range of potential C/O ratios is shown in Fig. 1. Two sources with non-detections could be interpreted as due to reduced C/O and we give that limit in the figure.

D. ADDITIONAL LANDSCAPE: GASEOUS DISK C/H

Another important aspect linking disk and exoplanet gas is the overall C/H ratios, for which there also are existing measurements. Again, we focus on measurements obtained beyond the CO_2 snowline. In this gas the expectation is that CO is the primary gas phase carbon carrier both inside and outside the CO snowline. That is in layers where the dust temperature is above the sublimation temperature of CO we anticipate that the abundance of CO would be $\sim 50\%$ of the solar value. The remaining 50% is found in refractory organic material (Pollack et al. 1994; Bergin et al. 2015).

A major complication in absolute abundance measurements is the estimation of the disk gaseous H_2 content. H_2 is unemissive in gas with temperatures $\sim 20-50$ K which encompasses the majority of the gas mass. At present the best method to determine the H_2 mass (see discussion in Bergin & Williams 2017; Miotello et al. 2022) is via HD emission (Bergin et al. 2013; McClure et al. 2016; Trapman et al. 2017), pressure broadening of CO emission (Yoshida et al. 2022b), gas kinematics (Paneque-Carreño et al. 2021), and N_2H^+ emission (Trapman et al. 2022; Anderson et al. 2022).

Based on these methods, current suggestions are that the disk gas phase C/H ratio is depleted relative to the expectations set by the interstellar medium/stellar (Favre et al. 2013; McClure et al. 2016; Schwarz et al. 2016; Zhang et al. 2017; Yoshida et al. 2022b; Trapman et al. 2022; Anderson et al. 2022) by factors of a few to 100 (Zhang et al. 2019). Of particular mention is the direct measurement of the H_2 density and (depleted) CO abundance in TW Hya inside of 20 au by Yoshida et al. (2022b). These are listed source by source in Appendix C. The central question is whether the carbon carried by CO is found on small grains in the form of less volatile species (Bergin et al. 2014; Furuya & Aikawa 2014; Reboussin et al. 2015; Eistrup et al. 2017; Schwarz et al. 2018; Bosman et al. 2018) or is carried (as ice) by successively larger grains to the dust-rich midplane (Xu et al. 2017; Krijt et al. 2018). This point matters in the context of the Öberg et al. (2011b) model as if CO were carried to the midplane by dust evolution (the latter solution) then it would be present in the solid planet cores. However, if CO is found in less volatile form on small grains then it would be accreted alongside the gas during the phase of gas capture. At present the situation is not clear. It is certain that the dust mass is concentrated in the midplane (Villenave et al. 2020) and the ice must be as well. Complex dust evolution models suggest dust evolution can matter and carry additional volatiles to the midplane (Krijt et al. 2020), but other analyses suggested otherwise (Ruaud et al. 2022; Pascucci et al. 2023). In our exploration we adopt C/H as a variable encompassing the range of highly depleted C/H (factor of 100) to relatively undepleted (factor of 2). This factor of 2 encompasses the fact that 50% of interstellar carbon is found in solid state carbonaceous grains (Mishra & Li 2015).

Table 1. Exoplanet Atmospheric Composition Measurements

Name	a (au)	M_p (M_{Jup})	C/O	σ (C/O)	C/H ^a	σ (C/H)	O/H ^a	σ (O/H)	References ^b
HR8799e	16.2	$7.5^{+0.6}_{-0.6}$	0.83	0.02	125.89	73.63	83.35	52.01	(1)
HR8799d	26.7	$9.2^{+0.1}_{-0.1}$	0.68	0.04	31.62	18.50	25.56	17.48	(1)
HR8799c	41.4	$8.5^{+0.4}_{-0.4}$	0.62	0.01	11.22	1.08	9.95	1.14	(1)
HR8799b	71.6	$6.0^{+0.3}_{-0.3}$	0.73	0.02	14.45	2.92	10.88	2.57	(1)
β Pic b	10.0	$9.3^{+2.6}_{-2.5}$	0.43	0.03	4.79	0.46	<i>6.12</i>	<i>1.09</i>	(2)
HIP65426b	92.0	$9.9^{+1.1}_{-1.8}$	<0.55	...	1.12	0.26	>1.12	...	(3)

^aAbundances given as absolute relative to solar, i.e. $(C/H)_{\text{planet}}/(C/H)_{\odot}$. Adopted solar values are $\log_{10}(C/H) = -3.57$ and $\log_{10}(O/H) = -3.31$ from [Asplund et al. \(2009\)](#). Values in italics were computed from the C/H and C/O quoted in the original references.

^b(1) [Nasedkin et al. \(2024\)](#). For masses adopt the single best fit retrieval parameters. (2) [GRAVITY Collaboration et al. \(2020\)](#); [Brandt et al. \(2021\)](#), (3) [Petrus et al. \(2021\)](#); [Wang \(2023\)](#)

E. EXOPLANET C/O RATIOS

We adopt recent measurements C/O and absolute abundances from a sample of direct detection planets including the four HR 8799 planets, β Pic b, and HIP 65426 b. These are listed with references in Table 1. For HR 8799 and β Pic b, the C/H abundances are derived from the metallicities, [M/H], given in the original references as the retrievals were done such that changes in the C/O changed the oxygen abundances only. Since [Petrus et al. \(2021\)](#) do not state whether [C/H], [O/H], or both were modified when changing the C/O ratio, we have assumed that C/H is given by [M/H]. The assumption is not critical for our analysis, however.

The abundances for the different planets have been determined from relatively homogeneous datasets. For HR 8799, we use the recent homogeneous analyses presented by [Nasedkin et al. \(2024\)](#) based on new GRAVITY data and supported by further data from SPHERE, GPI, CHARIS, OSIRIS, and ALES, and covering a wavelength range of 1–4 μ m. The β Pic b study is similarly based on GRAVITY data, combined with GPI Y, J, & H data and covers the range 1–2.5 μ m, as described by [GRAVITY Collaboration et al. \(2020\)](#). For HIP 65426 b, the data cover 1–4.7 μ m, including SPHERE IFS data from 1–1.5 μ m, SPHERE H band data, SINFONI K-band spectra and photometry in the L and M bands from NACO ([Petrus et al. 2021](#)). Note the analysis of HIP 65426 b by [Blunt et al. \(2023\)](#) that also includes GRAVITY data arrives at similar results ([M/H] \approx 0.15, [C/O] \approx 0.6).

The atmospheric compositions are derived from the spectra using a variety of different techniques: [Petrus et al. \(2021\)](#) use fits to grids of Exo-REM ([Baudino et al. 2015](#)) forward models to determine the abundances, while [GRAVITY Collaboration et al. \(2020\)](#) conduct both free retrievals with petitRADTRANS ([Mollière et al. 2019](#)) and forward models with Exo-REM, finding consistent results. [Nasedkin et al. \(2024\)](#) explore different methodologies for determining the abundances of the HR 8799 planets, including free retrievals, chemical (dis-)equilibrium retrievals and fits to grids of forward models. Their results highlight an important issue: cloud condensation can significantly affect the atmospheric C/O ratio as oxygen is locked into silicates, complicating the interpretation of the inferred abundances. In particular, the retrievals favor C/O ratios of 0.7–0.8, while the forward models are better fit with C/O ratios nearer solar (\approx 0.55).

Where possible, we adopt the results from retrieval analyses because the fits derived from a given forward model presented by [Nasedkin et al. \(2024\)](#) are quoted with uncertainties that are much smaller than the systematic differences between the different models. As a result, we use the free retrieval for β Pic-b, the dis-equilibrium chemistry retrieval for the HR 8799 system and the Exo-REM grid of forward models for HIP 65426 b. For HR 8799, we therefore correct the oxygen abundances in our planet formation models to account for the condensation of silicate clouds.

F. PLANET COMPOSITION MODEL

We adopt a simplified picture of planet formation where the bulk composition of the planets is computed by adding different amounts of gases and solids to the planet. We do not consider any radial variations in disc composition, so planet migration need not be considered. When comparing to the atmospheric composition we consider the impact of silicate cloud condensation on the observed abundances.

We need the composition of the gases and solids in the disc to compute the planet compositions. Starting from the [Asplund et al. \(2009\)](#) solar abundances, $X_{\odot,i}$ (the number of atoms of species i relative to the number of H atoms), we partition the abundances into the gas phase, $X_{g,i}$ and solid phase, $X_{s,i}$. We assume that hydrogen and all noble gases are entirely in the gas phase (i.e. $X_{g,i} = X_{\odot,i}$ when $i \in \{H, He, Ne, Xe, Ar\}$). For nitrogen, 90% is assumed to be in the gas-phase as N_2 (i.e. $X_{g,N} = 0.9X_{\odot,N}$). The gas-phase carbon and oxygen abundances are determined by the C/O ratio and the carbon depletion factor, Δ_C . Since approximately 50% of carbon in the ISM is in a refractory form ([Mishra & Li 2015](#)), we define $X_{g,C} = X_{\odot,C}/(2\Delta_C)$. The gas-phase oxygen abundance is then determined by the C/O ratio, $X_{g,O} = X_{g,C}/(C/O)$. No other species are considered to be in the gas phase.

The composition of the dust depends on whether the depletion of dust is considered. Without depletion, the total composition equates to solar so $X_{s,i} = X_{\odot,i} - X_{g,i}$.

When computing the abundance of solids after dust depletion, we need to know how much material is lost together with its composition. We assume that any dust evolution occurs while the disc has its initial composition as this maximizes the impact of dust evolution. We assume the composition is inherited from the ISM and that most of the volatile carbon is in the form of CO. Defining the initial gas- and solid-phase composition as $X_{g,i}^0$ and $X_{s,i}^0$, we can compute the $X_{g,i}^0$ by using $\Delta_C = 1$ and $C/O = 1$ in the expressions for $X_{g,i}$. Similarly, $X_{s,i}^0 = X_{\odot,i} - X_{g,i}^0$.

We assume that dust depletion reduces the dust mass by a factor Δ_d . As a result, the total gas+solid composition after dust depletion is $X_{g,i}^0 + X_{s,i}^0/\Delta_d$. Dust enhancement through traps can be modelled via $\Delta_d < 1$. Next, the disc composition evolves to its current state with a given C/O and level of carbon depletion. At this point $X_{s,i}$ can be computed from $X_{g,i}$ (itself calculated from Δ_C , C/O and $X_{\odot,i}$, as above) and the new total disc abundance via $X_{g,i} + X_{s,i} = X_{g,i}^0 + X_{s,i}^0/\Delta_d$. Any further evolution of the dust-to-gas ratio in the disc does not affect the range of planet abundances compatible with the disc model and is thus neglected.

The planet's bulk abundances, $X_{p,i}$ are constructed by adding different amounts of gas and solids, $X_{p,i} = X_{g,i} + fX_{s,i}$, with the factor f being varied to explore the different planet compositions compatible with the disc model. $f = 1$ corresponds to the case where the disc and planet composition are the same. Silicate cloud condensation is accounted for using the prescription from [Calamari et al. \(2024\)](#), in which condensation is estimated to reduce $X_{p,O}$ by $2.024X_{p,Si} + 1.167X_{p,Mg}$, equivalent to 3.45 oxygen atoms per silicon atom.

Finally, the mass fraction of solids accreted by the planet, f_s is computed via

$$f_s = \frac{\sum_i f X_{s,i} m_i}{\sum_i m_i (X_{g,i} + f X_{s,i})}, \quad (F1)$$

where m_i is mass of the species. Note that silicates are included in $X_{p,O}$ when computing f_s .

REFERENCES

- Aikawa, Y., van Zadelhoff, G. J., van Dishoeck, E. F., & Herbst, E. 2002, *A&A*, 386, 622, doi: [10.1051/0004-6361:20020037](https://doi.org/10.1051/0004-6361:20020037)
- Alarcón, F., Bosman, A. D., Bergin, E. A., et al. 2021, *ApJS*, 257, 8, doi: [10.3847/1538-4365/ac22ae](https://doi.org/10.3847/1538-4365/ac22ae)
- Alcalá, J. M., Manara, C. F., Natta, A., et al. 2017, *A&A*, 600, A20, doi: [10.1051/0004-6361/201629929](https://doi.org/10.1051/0004-6361/201629929)
- Anderson, D. E., Cleeves, L. I., Blake, G. A., et al. 2022, *ApJ*, 927, 229, doi: [10.3847/1538-4357/ac517e](https://doi.org/10.3847/1538-4357/ac517e)
- Andrews, S. M. 2020, *ARA&A*, 58, 483, doi: [10.1146/annurev-astro-031220-010302](https://doi.org/10.1146/annurev-astro-031220-010302)
- Andrews, S. M., Huang, J., Pérez, L. M., et al. 2018, *ApJL*, 869, L41, doi: [10.3847/2041-8213/aaf741](https://doi.org/10.3847/2041-8213/aaf741)
- Ansdell, M., Williams, J. P., van der Marel, N., et al. 2016, *ApJ*, 828, 46, doi: [10.3847/0004-637X/828/1/46](https://doi.org/10.3847/0004-637X/828/1/46)
- Ansdell, M., Williams, J. P., Trapman, L., et al. 2018, *ApJ*, 859, 21, doi: [10.3847/1538-4357/aab890](https://doi.org/10.3847/1538-4357/aab890)
- Artur de la Villarmois, E., Guzmán, V. V., Jørgensen, J. K., et al. 2022, *A&A*, 667, A20, doi: [10.1051/0004-6361/202244312](https://doi.org/10.1051/0004-6361/202244312)
- Asplund, M., Amarsi, A. M., & Grevesse, N. 2021, *A&A*, 653, A141, doi: [10.1051/0004-6361/202140445](https://doi.org/10.1051/0004-6361/202140445)
- Asplund, M., Grevesse, N., Sauval, A. J., & Scott, P. 2009, *ARA&A*, 47, 481, doi: [10.1146/annurev.astro.46.060407.145222](https://doi.org/10.1146/annurev.astro.46.060407.145222)
- Astropy Collaboration, Robitaille, T. P., Tollerud, E. J., et al. 2013, *A&A*, 558, A33, doi: [10.1051/0004-6361/201322068](https://doi.org/10.1051/0004-6361/201322068)
- Astropy Collaboration, Price-Whelan, A. M., Sipőcz, B. M., et al. 2018, *AJ*, 156, 123, doi: [10.3847/1538-3881/aabc4f](https://doi.org/10.3847/1538-3881/aabc4f)
- Avenhaus, H., Quanz, S. P., Garufi, A., et al. 2018, *ApJ*, 863, 44, doi: [10.3847/1538-4357/aab846](https://doi.org/10.3847/1538-4357/aab846)
- Bae, J., Isella, A., Zhu, Z., et al. 2023, in *Astronomical Society of the Pacific Conference Series*, Vol. 534, *Protostars and Planets VII*, ed. S. Inutsuka, Y. Aikawa, T. Muto, K. Tomida, & M. Tamura, 423, doi: [10.48550/arXiv.2210.13314](https://doi.org/10.48550/arXiv.2210.13314)

- Barman, T. S., Konopacky, Q. M., Macintosh, B., & Marois, C. 2015, *ApJ*, 804, 61, doi: [10.1088/0004-637X/804/1/61](https://doi.org/10.1088/0004-637X/804/1/61)
- Baudino, J. L., Bézard, B., Boccaletti, A., et al. 2015, *A&A*, 582, A83, doi: [10.1051/0004-6361/201526332](https://doi.org/10.1051/0004-6361/201526332)
- Bergemann, M., Hoppe, R., Seménova, E., et al. 2021, *MNRAS*, 508, 2236, doi: [10.1093/mnras/stab2160](https://doi.org/10.1093/mnras/stab2160)
- Bergin, E. A., Blake, G. A., Ciesla, F., Hirschmann, M. M., & Li, J. 2015, *Proceedings of the National Academy of Science*, 112, 8965, doi: [10.1073/pnas.1500954112](https://doi.org/10.1073/pnas.1500954112)
- Bergin, E. A., Cleeves, L. I., Crockett, N., & Blake, G. A. 2014, *Faraday Discuss.*, 168, 61, doi: [10.1039/C4FD00003J](https://doi.org/10.1039/C4FD00003J)
- Bergin, E. A., Du, F., Cleeves, L. I., et al. 2016, *ApJ*, 831, 101, doi: [10.3847/0004-637X/831/1/101](https://doi.org/10.3847/0004-637X/831/1/101)
- Bergin, E. A., Goldsmith, P. F., Snell, R. L., & Langer, W. D. 1997, *ApJ*, 482, 285, doi: [10.1086/304108](https://doi.org/10.1086/304108)
- Bergin, E. A., & Williams, J. P. 2017, *Formation, Evolution, and Dynamics of Young Solar Systems*, 445, in press
- Bergin, E. A., Cleeves, L. I., Gorti, U., et al. 2013, *Nature*, 493, 644, doi: [10.1038/nature11805](https://doi.org/10.1038/nature11805)
- Bergner, J. B., Martín-Doménech, R., Öberg, K. I., et al. 2019, *ACS Earth and Space Chemistry*, 3, 1564, doi: [10.1021/acsearthspacechem.9b00059](https://doi.org/10.1021/acsearthspacechem.9b00059)
- Biazzo, K., D’Orazi, V., Desidera, S., et al. 2022, *A&A*, 664, A161, doi: [10.1051/0004-6361/202243467](https://doi.org/10.1051/0004-6361/202243467)
- Birnstiel, T., Dullemond, C. P., Zhu, Z., et al. 2018, *ApJL*, 869, L45, doi: [10.3847/2041-8213/aaf743](https://doi.org/10.3847/2041-8213/aaf743)
- Bitsch, B., Morbidelli, A., Johansen, A., et al. 2018, *A&A*, 612, A30, doi: [10.1051/0004-6361/201731931](https://doi.org/10.1051/0004-6361/201731931)
- Blunt, S., Balmer, W. O., Wang, J. J., et al. 2023, *AJ*, 166, 257, doi: [10.3847/1538-3881/ad06b7](https://doi.org/10.3847/1538-3881/ad06b7)
- Boley, A. C., & Durisen, R. H. 2010, *ApJ*, 724, 618, doi: [10.1088/0004-637X/724/1/618](https://doi.org/10.1088/0004-637X/724/1/618)
- Booth, A. S., Ilee, J. D., Walsh, C., et al. 2023, *A&A*, 669, A53, doi: [10.1051/0004-6361/202244472](https://doi.org/10.1051/0004-6361/202244472)
- Booth, R. A., Clarke, C. J., Madhusudhan, N., & Ilee, J. D. 2017, *MNRAS*, 469, 3994, doi: [10.1093/mnras/stx1103](https://doi.org/10.1093/mnras/stx1103)
- Booth, R. A., & Ilee, J. D. 2019, *MNRAS*, 487, 3998, doi: [10.1093/mnras/stz1488](https://doi.org/10.1093/mnras/stz1488)
- Bosman, A. D., Alarcón, F., Zhang, K., & Bergin, E. A. 2021a, *ApJ*, 910, 3, doi: [10.3847/1538-4357/abe127](https://doi.org/10.3847/1538-4357/abe127)
- Bosman, A. D., & Banzatti, A. 2019, *A&A*, 632, L10, doi: [10.1051/0004-6361/201936638](https://doi.org/10.1051/0004-6361/201936638)
- Bosman, A. D., Bergin, E. A., Calahan, J., & Duval, S. E. 2022, *arXiv e-prints*, arXiv:2204.07108, <https://arxiv.org/abs/2204.07108>
- Bosman, A. D., Walsh, C., & van Dishoeck, E. F. 2018, *A&A*, 618, A182, doi: [10.1051/0004-6361/201833497](https://doi.org/10.1051/0004-6361/201833497)
- Bosman, A. D., Bergin, E. A., Loomis, R. A., et al. 2021b, *ApJS*, 257, 15, doi: [10.3847/1538-4365/ac1433](https://doi.org/10.3847/1538-4365/ac1433)
- Boss, A. P. 1997, *Science*, 276, 1836, doi: [10.1126/science.276.5320.1836](https://doi.org/10.1126/science.276.5320.1836)
- Brandt, G. M., Brandt, T. D., Dupuy, T. J., Li, Y., & Michalik, D. 2021, *AJ*, 161, 179, doi: [10.3847/1538-3881/abcd2e](https://doi.org/10.3847/1538-3881/abcd2e)
- Bruderer, S., van Dishoeck, E. F., Doty, S. D., & Herczeg, G. J. 2012, *A&A*, 541, A91, doi: [10.1051/0004-6361/201118218](https://doi.org/10.1051/0004-6361/201118218)
- Calahan, J. K., Bergin, E., Zhang, K., et al. 2021, *ApJ*, 908, 8, doi: [10.3847/1538-4357/abd255](https://doi.org/10.3847/1538-4357/abd255)
- Calahan, J. K., Bergin, E. A., Bosman, A. D., et al. 2023, *Nature Astronomy*, 7, 49, doi: [10.1038/s41550-022-01831-8](https://doi.org/10.1038/s41550-022-01831-8)
- Calamari, E., Faherty, J. K., Visscher, C., et al. 2024, *ApJ*, 963, 67, doi: [10.3847/1538-4357/ad1f6d](https://doi.org/10.3847/1538-4357/ad1f6d)
- Carr, J. S., & Najita, J. R. 2011, *ApJ*, 733, 102, doi: [10.1088/0004-637X/733/2/102](https://doi.org/10.1088/0004-637X/733/2/102)
- Cleeves, L. I., Adams, F. C., & Bergin, E. A. 2013, *ApJ*, 772, 5, doi: [10.1088/0004-637X/772/1/5](https://doi.org/10.1088/0004-637X/772/1/5)
- Cleeves, L. I., Öberg, K. I., Wilner, D. J., et al. 2016, *ApJ*, 832, 110, doi: [10.3847/0004-637X/832/2/110](https://doi.org/10.3847/0004-637X/832/2/110)
- . 2018, *ApJ*, 865, 155, doi: [10.3847/1538-4357/aade96](https://doi.org/10.3847/1538-4357/aade96)
- Cleeves, L. I., Loomis, R. A., Teague, R., et al. 2021, *ApJ*, 911, 29, doi: [10.3847/1538-4357/abe862](https://doi.org/10.3847/1538-4357/abe862)
- Cridland, A. J., Pudritz, R. E., & Birnstiel, T. 2016, *MNRAS*, submitted
- Currie, T., Lawson, K., Schneider, G., et al. 2022, *Nature Astronomy*, 6, 751, doi: [10.1038/s41550-022-01634-x](https://doi.org/10.1038/s41550-022-01634-x)
- Danti, C., Bitsch, B., & Mah, J. 2023, *A&A*, 679, L7, doi: [10.1051/0004-6361/202347501](https://doi.org/10.1051/0004-6361/202347501)
- Debes, J. H., Jang-Condell, H., Weinberger, A. J., Roberge, A., & Schneider, G. 2013, *ApJ*, 771, 45, doi: [10.1088/0004-637X/771/1/45](https://doi.org/10.1088/0004-637X/771/1/45)
- Donati, J. F., Bouvier, J., Alencar, S. H., et al. 2019, *MNRAS*, 483, L1, doi: [10.1093/mnras/sly207](https://doi.org/10.1093/mnras/sly207)
- Du, F., & Bergin, E. A. 2014, *ApJ*, 792, 2, doi: [10.1088/0004-637X/792/1/2](https://doi.org/10.1088/0004-637X/792/1/2)
- Durisen, R. H., Boss, A. P., Mayer, L., et al. 2007, in *Protostars and Planets V*, ed. B. Reipurth, D. Jewitt, & K. Keil, 607, doi: [10.48550/arXiv.astro-ph/0603179](https://doi.org/10.48550/arXiv.astro-ph/0603179)
- Dutrey, A., Guilloteau, S., Piétu, V., et al. 2017, *A&A*, 607, A130, doi: [10.1051/0004-6361/201730645](https://doi.org/10.1051/0004-6361/201730645)
- Eistrup, C., Walsh, C., & van Dishoeck, E. F. 2017, *A&A*, in press
- Facchini, S., Benisty, M., Bae, J., et al. 2020, *A&A*, 639, A121, doi: [10.1051/0004-6361/202038027](https://doi.org/10.1051/0004-6361/202038027)
- Fairlamb, J. R., Oudmaijer, R. D., Mendigutía, I., Ilee, J. D., & van den Ancker, M. E. 2015, *MNRAS*, 453, 976, doi: [10.1093/mnras/stv1576](https://doi.org/10.1093/mnras/stv1576)
- Favre, C., Cleeves, L. I., Bergin, E. A., Qi, C., & Blake, G. A. 2013, *ApJL*, 776, L38, doi: [10.1088/2041-8205/776/2/L38](https://doi.org/10.1088/2041-8205/776/2/L38)
- Fedele, D., & Favre, C. 2020, *A&A*, 638, A110, doi: [10.1051/0004-6361/202037927](https://doi.org/10.1051/0004-6361/202037927)

- Flores, C., Ohashi, N., Tobin, J. J., et al. 2023, *ApJ*, 958, 98, doi: [10.3847/1538-4357/acf7c1](https://doi.org/10.3847/1538-4357/acf7c1)
- Furuya, K., & Aikawa, Y. 2014, *ApJ*, 790, 97, doi: [10.1088/0004-637X/790/2/97](https://doi.org/10.1088/0004-637X/790/2/97)
- Gaia Collaboration, Brown, A. G. A., Vallenari, A., et al. 2016, *A&A*, 595, A2, doi: [10.1051/0004-6361/201629512](https://doi.org/10.1051/0004-6361/201629512)
- . 2018, *A&A*, 616, A1, doi: [10.1051/0004-6361/201833051](https://doi.org/10.1051/0004-6361/201833051)
- Gorti, U., Hollenbach, D., Najita, J., & Pascucci, I. 2011, *ApJ*, 735, 90, doi: [10.1088/0004-637X/735/2/90](https://doi.org/10.1088/0004-637X/735/2/90)
- GRAVITY Collaboration, Nowak, M., Lacour, S., et al. 2020, *A&A*, 633, A110, doi: [10.1051/0004-6361/201936898](https://doi.org/10.1051/0004-6361/201936898)
- Guillot, T., Fletcher, L. N., Helled, R., et al. 2022, arXiv e-prints, arXiv:2205.04100. <https://arxiv.org/abs/2205.04100>
- Guzmán, V. V., Bergner, J. B., Law, C. J., et al. 2021, *ApJS*, 257, 6, doi: [10.3847/1538-4365/ac1440](https://doi.org/10.3847/1538-4365/ac1440)
- Guzmán-Díaz, J., Mendigutía, I., Montesinos, B., et al. 2021, *A&A*, 650, A182, doi: [10.1051/0004-6361/202039519](https://doi.org/10.1051/0004-6361/202039519)
- Harsono, D., Bruderer, S., & van Dishoeck, E. F. 2015, *A&A*, 582, A41, doi: [10.1051/0004-6361/201525966](https://doi.org/10.1051/0004-6361/201525966)
- Helled, R., & Guillot, T. 2017, in *Handbook of Exoplanets*. <https://arxiv.org/abs/1705.09320>
- Herczeg, G. J., & Hillenbrand, L. A. 2014, *ApJ*, 786, 97, doi: [10.1088/0004-637X/786/2/97](https://doi.org/10.1088/0004-637X/786/2/97)
- Huang, J., Andrews, S. M., Dullemond, C. P., et al. 2018, *ApJL*, 869, L42, doi: [10.3847/2041-8213/aaf740](https://doi.org/10.3847/2041-8213/aaf740)
- Ilee, J. D., Forgan, D. H., Evans, M. G., et al. 2017, *MNRAS*, 472, 189, doi: [10.1093/mnras/stx1966](https://doi.org/10.1093/mnras/stx1966)
- Ilee, J. D., Walsh, C., Booth, A. S., et al. 2021, *ApJS*, 257, 9, doi: [10.3847/1538-4365/ac1441](https://doi.org/10.3847/1538-4365/ac1441)
- Kalyaan, A., Pinilla, P., Krijt, S., et al. 2023, *ApJ*, 954, 66, doi: [10.3847/1538-4357/ace535](https://doi.org/10.3847/1538-4357/ace535)
- Kama, M., Bruderer, S., van Dishoeck, E. F., et al. 2016, *A&A*, in press.
- Kastner, J. H., Hily-Blant, P., Rodriguez, D. R., Punzi, K., & Forveille, T. 2014, *ApJ*, 793, 55, doi: [10.1088/0004-637X/793/1/55](https://doi.org/10.1088/0004-637X/793/1/55)
- Kastner, J. H., Qi, C., Gorti, U., et al. 2015, *ApJ*, 806, 75, doi: [10.1088/0004-637X/806/1/75](https://doi.org/10.1088/0004-637X/806/1/75)
- Keyte, L., Kama, M., Booth, A. S., et al. 2023, *Nature Astronomy*, 7, 684, doi: [10.1038/s41550-023-01951-9](https://doi.org/10.1038/s41550-023-01951-9)
- Kido, M., Takakuwa, S., Saigo, K., et al. 2023, *ApJ*, 953, 190, doi: [10.3847/1538-4357/acdd7a](https://doi.org/10.3847/1538-4357/acdd7a)
- Krijt, S., Bosman, A. D., Zhang, K., et al. 2020, *ApJ*, 899, 134, doi: [10.3847/1538-4357/aba75d](https://doi.org/10.3847/1538-4357/aba75d)
- Krijt, S., Schwarz, K. R., Bergin, E. A., & Ciesla, F. J. 2018, *ApJ*, 864, 78, doi: [10.3847/1538-4357/aad69b](https://doi.org/10.3847/1538-4357/aad69b)
- Lavie, B., Mendonça, J. M., Mordasini, C., et al. 2017, *AJ*, 154, 91, doi: [10.3847/1538-3881/aa7ed8](https://doi.org/10.3847/1538-3881/aa7ed8)
- Law, C. J., Loomis, R. A., Teague, R., et al. 2021, *ApJS*, 257, 3, doi: [10.3847/1538-4365/ac1434](https://doi.org/10.3847/1538-4365/ac1434)
- Le Gal, R., Öberg, K. I., Teague, R., et al. 2021, *ApJS*, 257, 12, doi: [10.3847/1538-4365/ac2583](https://doi.org/10.3847/1538-4365/ac2583)
- Lee, S., Nomura, H., Furuya, K., & Lee, J.-E. 2021, *ApJ*, 908, 82, doi: [10.3847/1538-4357/abd633](https://doi.org/10.3847/1538-4357/abd633)
- McClure, M. K., Dominik, C., & Kama, M. 2020, *A&A*, 642, L15, doi: [10.1051/0004-6361/202038912](https://doi.org/10.1051/0004-6361/202038912)
- McClure, M. K., Bergin, E. A., Cleeves, L. I., et al. 2016, *ApJ*, 831, 167, doi: [10.3847/0004-637X/831/2/167](https://doi.org/10.3847/0004-637X/831/2/167)
- McClure, M. K., Rocha, W. R. M., Pontoppidan, K. M., et al. 2023, *Nature Astronomy*, 7, 431, doi: [10.1038/s41550-022-01875-w](https://doi.org/10.1038/s41550-022-01875-w)
- Minissale, M., Aikawa, Y., Bergin, E., et al. 2022, *ACS Earth and Space Chemistry*, 6, 597, doi: [10.1021/acsearthspacechem.1c00357](https://doi.org/10.1021/acsearthspacechem.1c00357)
- Miotello, A., Kamp, I., Birnstiel, T., Cleeves, L. I., & Kataoka, A. 2022, arXiv e-prints, arXiv:2203.09818. <https://arxiv.org/abs/2203.09818>
- Miotello, A., Facchini, S., van Dishoeck, E. F., et al. 2019, *A&A*, 631, A69, doi: [10.1051/0004-6361/201935441](https://doi.org/10.1051/0004-6361/201935441)
- Mishra, A., & Li, A. 2015, *ApJ*, 809, 120, doi: [10.1088/0004-637X/809/2/120](https://doi.org/10.1088/0004-637X/809/2/120)
- Miura, H., Yamamoto, T., Nomura, H., et al. 2017, *ApJ*, 839, 47, doi: [10.3847/1538-4357/aa67df](https://doi.org/10.3847/1538-4357/aa67df)
- Mollière, P., Wardenier, J. P., van Boekel, R., et al. 2019, *A&A*, 627, A67, doi: [10.1051/0004-6361/201935470](https://doi.org/10.1051/0004-6361/201935470)
- Mollière, P., Stolker, T., Lacour, S., et al. 2020, *A&A*, 640, A131, doi: [10.1051/0004-6361/202038325](https://doi.org/10.1051/0004-6361/202038325)
- Montesinos, B., Eiroa, C., Mora, A., & Merín, B. 2009, *A&A*, 495, 901, doi: [10.1051/0004-6361:200810623](https://doi.org/10.1051/0004-6361:200810623)
- Mordasini, C., van Boekel, R., Mollière, P., Henning, T., & Benneke, B. 2016, *ApJ*, 832, 41, doi: [10.3847/0004-637X/832/1/41](https://doi.org/10.3847/0004-637X/832/1/41)
- Nagy, Z., Ossenkopf, V., Van der Tak, F. F. S., et al. 2015, *A&A*, 578, A124, doi: [10.1051/0004-6361/201424220](https://doi.org/10.1051/0004-6361/201424220)
- Nasedkin, E., Mollière, P., Lacour, S., et al. 2024, *â*, submitted, doi: [10.48550/arXiv.2404.03776](https://doi.org/10.48550/arXiv.2404.03776)
- Nayakshin, S. 2010, *MNRAS*, 408, L36, doi: [10.1111/j.1745-3933.2010.00923.x](https://doi.org/10.1111/j.1745-3933.2010.00923.x)
- Nieva, M. F., & Przybilla, N. 2012, *Astronomy and Astrophysics*, 539, A143
- Nilsson, A., Hjalmarson, Å., Bergman, P., & Millar, T. J. 2000, *A&A*, 358, 257
- Öberg, K. I., & Bergin, E. A. 2021, *PhR*, 893, 1, doi: [10.1016/j.physrep.2020.09.004](https://doi.org/10.1016/j.physrep.2020.09.004)
- Öberg, K. I., Boogert, A. C. A., Pontoppidan, K. M., et al. 2011a, *ApJ*, 740, 109, doi: [10.1088/0004-637X/740/2/109](https://doi.org/10.1088/0004-637X/740/2/109)
- Öberg, K. I., Murray-Clay, R., & Bergin, E. A. 2011b, *ApJL*, 743, L16, doi: [10.1088/2041-8205/743/1/L16](https://doi.org/10.1088/2041-8205/743/1/L16)
- Öberg, K. I., Guzmán, V. V., Walsh, C., et al. 2021, *ApJS*, 257, 1, doi: [10.3847/1538-4365/ac1432](https://doi.org/10.3847/1538-4365/ac1432)

- Oreshenko, M., Lavie, B., Grimm, S. L., et al. 2017, *ApJL*, 847, L3, doi: [10.3847/2041-8213/aa8acf](https://doi.org/10.3847/2041-8213/aa8acf)
- Ormel, C. W., Vazan, A., & Brouwers, M. G. 2021, *A&A*, 647, A175, doi: [10.1051/0004-6361/202039706](https://doi.org/10.1051/0004-6361/202039706)
- Pacheco-Vázquez, S., Fuente, A., Baruteau, C., et al. 2016, *A&A*, 589, A60, doi: [10.1051/0004-6361/201527089](https://doi.org/10.1051/0004-6361/201527089)
- Paneque-Carreño, T., Pérez, L. M., Benisty, M., et al. 2021, *ApJ*, 914, 88, doi: [10.3847/1538-4357/abf243](https://doi.org/10.3847/1538-4357/abf243)
- Pascucci, I., Skinner, B. N., Deng, D., et al. 2023, *ApJ*, 953, 183, doi: [10.3847/1538-4357/ace4bf](https://doi.org/10.3847/1538-4357/ace4bf)
- Pegues, J., Öberg, K. I., Bergner, J. B., et al. 2020, *ApJ*, 890, 142, doi: [10.3847/1538-4357/ab64d9](https://doi.org/10.3847/1538-4357/ab64d9)
- Petrus, S., Bonnefoy, M., Chauvin, G., et al. 2021, *A&A*, 648, A59, doi: [10.1051/0004-6361/202038914](https://doi.org/10.1051/0004-6361/202038914)
- Piétu, V., Dutrey, A., Guilloteau, S., Chapillon, E., & Pety, J. 2006, *A&A*, 460, L43, doi: [10.1051/0004-6361:20065968](https://doi.org/10.1051/0004-6361:20065968)
- Pinilla, P., Pohl, A., Stammer, S. M., & Birnstiel, T. 2017, *ApJ*, 845, 68, doi: [10.3847/1538-4357/aa7edb](https://doi.org/10.3847/1538-4357/aa7edb)
- Pinte, C., Teague, R., Flaherty, K., et al. 2023, in *Astronomical Society of the Pacific Conference Series*, Vol. 534, *Protostars and Planets VII*, ed. S. Inutsuka, Y. Aikawa, T. Muto, K. Tomida, & M. Tamura, 645, doi: [10.48550/arXiv.2203.09528](https://doi.org/10.48550/arXiv.2203.09528)
- Pinte, C., Padgett, D. L., Ménard, F., et al. 2008, *A&A*, 489, 633, doi: [10.1051/0004-6361:200810121](https://doi.org/10.1051/0004-6361:200810121)
- Pollack, J. B., Hollenbach, D., Beckwith, S., et al. 1994, *ApJ*, 421, 615, doi: [10.1086/173677](https://doi.org/10.1086/173677)
- Pollack, J. B., Kasting, J. F., Richardson, S. M., & Poliakoff, K. 1987, *Icarus*, 71, 203, doi: [10.1016/0019-1035\(87\)90147-3](https://doi.org/10.1016/0019-1035(87)90147-3)
- Qi, C., Öberg, K. I., Espaillat, C. C., et al. 2019, *ApJ*, 882, 160, doi: [10.3847/1538-4357/ab35d3](https://doi.org/10.3847/1538-4357/ab35d3)
- Reboussin, L., Wakelam, V., Guilloteau, S., Hersant, F., & Dutrey, A. 2015, *A&A*, 579, A82, doi: [10.1051/0004-6361/201525885](https://doi.org/10.1051/0004-6361/201525885)
- Rivière-Marichalar, P., Fuente, A., Le Gal, R., et al. 2020, *A&A*, 642, A32, doi: [10.1051/0004-6361/202038549](https://doi.org/10.1051/0004-6361/202038549)
- Rivière-Marichalar, P., Fuente, A., Esplugues, G., et al. 2022, *A&A*, 665, A61, doi: [10.1051/0004-6361/202142906](https://doi.org/10.1051/0004-6361/202142906)
- Ruud, M., Gorti, U., & Hollenbach, D. J. 2022, *ApJ*, 925, 49, doi: [10.3847/1538-4357/ac3826](https://doi.org/10.3847/1538-4357/ac3826)
- Ruffio, J.-B., Konopacky, Q. M., Barman, T., et al. 2021, *AJ*, 162, 290, doi: [10.3847/1538-3881/ac273a](https://doi.org/10.3847/1538-3881/ac273a)
- Sakai, N., Sakai, T., Hirota, T., et al. 2014, *Nature*, 507, 78, doi: [10.1038/nature13000](https://doi.org/10.1038/nature13000)
- Sanchis, E., Testi, L., Natta, A., et al. 2021, *A&A*, 649, A19, doi: [10.1051/0004-6361/202039733](https://doi.org/10.1051/0004-6361/202039733)
- Schwarz, K. R., Bergin, E. A., Cleeves, L. I., et al. 2016, *ApJ*, 823, 91, doi: [10.3847/0004-637X/823/2/91](https://doi.org/10.3847/0004-637X/823/2/91)
- . 2018, *ApJ*, 856, 85, doi: [10.3847/1538-4357/aaae08](https://doi.org/10.3847/1538-4357/aaae08)
- Semenov, D., Favre, C., Fedele, D., et al. 2018, *A&A*, 617, A28, doi: [10.1051/0004-6361/201832980](https://doi.org/10.1051/0004-6361/201832980)
- Simon, M., Guilloteau, S., Beck, T. L., et al. 2019, *ApJ*, 884, 42, doi: [10.3847/1538-4357/ab3e3b](https://doi.org/10.3847/1538-4357/ab3e3b)
- Sokal, K. R., Deen, C. P., Mace, G. N., et al. 2018, *ApJ*, 853, 120, doi: [10.3847/1538-4357/aaa1e4](https://doi.org/10.3847/1538-4357/aaa1e4)
- Sturm, J. A., Booth, A. S., McClure, M. K., Leemker, M., & van Dishoeck, E. F. 2022, arXiv e-prints, arXiv:2209.09286. <https://arxiv.org/abs/2209.09286>
- Tang, Y. W., Guilloteau, S., Piétu, V., et al. 2012, *A&A*, 547, A84, doi: [10.1051/0004-6361/201219414](https://doi.org/10.1051/0004-6361/201219414)
- Thorngren, D. P., Fortney, J. J., Murray-Clay, R. A., & Lopez, E. D. 2016, *ApJ*, 831, 64, doi: [10.3847/0004-637X/831/1/64](https://doi.org/10.3847/0004-637X/831/1/64)
- Trapman, L., Miotello, A., Kama, M., van Dishoeck, E. F., & Bruderer, S. 2017, *A&A*, 605, A69, doi: [10.1051/0004-6361/201630308](https://doi.org/10.1051/0004-6361/201630308)
- Trapman, L., Zhang, K., van't Hoff, M. L. R., Hogerheijde, M. R., & Bergin, E. A. 2022, *ApJL*, 926, L2, doi: [10.3847/2041-8213/ac4f47](https://doi.org/10.3847/2041-8213/ac4f47)
- Umebayashi, T., & Nakano, T. 1988, *Progress of Theoretical Physics Supplement*, 96, 151, doi: [10.1143/PTPS.96.151](https://doi.org/10.1143/PTPS.96.151)
- van Gelder, M. L., Tabone, B., van Dishoeck, E. F., & Godard, B. 2021, *A&A*, 653, A159, doi: [10.1051/0004-6361/202141591](https://doi.org/10.1051/0004-6361/202141591)
- Villeneuve, M., Ménard, F., Dent, W. R. F., et al. 2020, *A&A*, 642, A164, doi: [10.1051/0004-6361/202038087](https://doi.org/10.1051/0004-6361/202038087)
- Wang, J. 2023, *AJ*, 166, 203, doi: [10.3847/1538-3881/acfca0](https://doi.org/10.3847/1538-3881/acfca0)
- Wang, J., Wang, J. J., Ma, B., et al. 2020, *AJ*, 160, 150, doi: [10.3847/1538-3881/ababa7](https://doi.org/10.3847/1538-3881/ababa7)
- Woitke, P., Kamp, I., & Thi, W.-F. 2009, *A&A*, 501, 383, doi: [10.1051/0004-6361/200911821](https://doi.org/10.1051/0004-6361/200911821)
- Xu, R., Bai, X.-N., & Öberg, K. 2017, *ApJ*, 835, 162, doi: [10.3847/1538-4357/835/2/162](https://doi.org/10.3847/1538-4357/835/2/162)
- Yoshida, T. C., Nomura, H., Furuya, K., Tsukagoshi, T., & Lee, S. 2022a, *ApJ*, 932, 126, doi: [10.3847/1538-4357/ac6efb](https://doi.org/10.3847/1538-4357/ac6efb)
- Yoshida, T. C., Nomura, H., Tsukagoshi, T., Furuya, K., & Ueda, T. 2022b, *ApJL*, 937, L14, doi: [10.3847/2041-8213/ac903a](https://doi.org/10.3847/2041-8213/ac903a)
- Zhang, K., Bergin, E. A., Blake, G. A., Cleeves, L. I., & Schwarz, K. R. 2017, *Nature Astronomy*, 1, 0130, doi: [10.1038/s41550-017-0130](https://doi.org/10.1038/s41550-017-0130)
- Zhang, K., Bergin, E. A., Schwarz, K., Krijt, S., & Ciesla, F. 2019, *ApJ*, 883, 98, doi: [10.3847/1538-4357/ab38b9](https://doi.org/10.3847/1538-4357/ab38b9)
- Zhang, K., Bosman, A. D., & Bergin, E. A. 2020, *ApJL*, 891, L16, doi: [10.3847/2041-8213/ab77ca](https://doi.org/10.3847/2041-8213/ab77ca)
- Zhang, K., Booth, A. S., Law, C. J., et al. 2021, *ApJS*, 257, 5, doi: [10.3847/1538-4365/ac1580](https://doi.org/10.3847/1538-4365/ac1580)